ACCOUNTS
of chemical research

Oxide Contacts in Organic Photovoltaics: Characterization and Control of Near-Surface Composition in Indium−Tin Oxide (ITO) Electrodes

NEAL R. ARMSTRONG,*,† P. ALEX VENEMAN,† ERIN RATCLIFF,† DIOGENES PLACENCIA,† AND MICHAEL BRUMBACH‡

†Department of Chemistry, University of Arizona, Tucson, Arizona 85721, ‡Sandia National Laboratories, Albuquerque, New Mexico 87185

RECEIVED ON APRIL 9, 2009

CONSPECTUS

The recent improvements in the power conversion efficiencies of organic photovoltaic devices (OPVs) promise to make these technologies increasingly attractive alternatives to more established photovoltaic technologies. OPVs typically consist of photoactive layers 20−100 nm thick sandwiched between both transparent oxide and metallic electrical contacts. Ideal OPVs rely on ohmic top and bottom contacts to harvest photogenerated charges without compromising the power conversion efficiency of the OPV. Unfortunately, the electrical contact materials (metals and metal oxides) and the active organic layers in OPVs are often incompatible and may be poorly optimized for harvesting photogenerated charges. Therefore, further optimization of the chemical and physical stabilities of these metal oxide materials with organic materials will be an essential component of the development of OPV technologies. The energetic and kinetic barriers to charge injection/collection must be minimized to maximize OPV power conversion efficiencies.

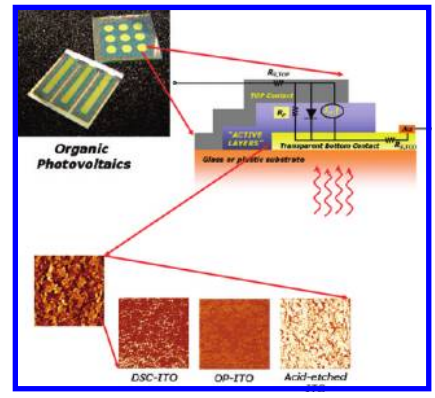

In this Account, we review recent studies of one of the most common transparent conducting oxides (TCOs), indium−tin oxide (ITO), which is the transparent bottom contact in many OPV technologies. These studies of the surface chemistry and surface modification of ITO are also applicable to other TCO materials. Clean, freshly deposited ITO is intrinsically reactive toward H_2O, CO, CO_2, etc. and is often chemically and electrically heterogeneous in the near-surface region. Conductive-tip atomic force microscopy (C-AFM) studies reveal significant spatial variability in electrical properties. We describe the use of acid activation, small-molecule chemisorption, and electrodeposition of conducting polymer films to tune the surface free energy, the effective work function, and electrochemical reactivity of ITO surfaces. Certain electrodeposited poly(thiophenes) show their own photovoltaic activity or can be used as electronically tunable substrates for other photoactive layers. For certain photoactive donor layers (phthalocyanines), we have used the polarity of the oxide surface to accelerate dewetting and "nanotexturing" of the donor layer to enhance OPV performance. These complex surface chemistries will make oxide/organic interfaces one of the key focal points for research in new OPV technologies.

Introduction

Recent improvements in the efficiency of organic photovoltaic devices (OPVs) are impressive.[1−11] Increases in power conversion efficiencies (η) in OPVs must be preceded by (i) the development of new light-absorbing (nanotextured) materials, (ii) better understandings of photo-induced electron transfer (PIET), exciton diffusion, and charge migration in organic solids, and (iii) control of factors that limit efficient charge collection at both metal and metal oxide contacts. This Account focuses on indium−tin oxide (ITO), the most prominent transparent conducting oxide (TCO) OPV contact. Optimizing the chemical and physical stabilities of the interfaces of these oxides with organic materials is essential to OPV development.[12−14]

Published on the Web 09/03/2009 www.pubs.acs.org/acr
10.1021/ar900096f CCC: $71.50

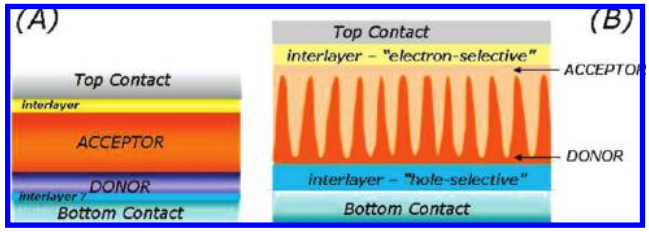

FIGURE 1. Schematic views of (A) planar heterojunction (PHJ) OPVs and (B) ideal blended heterojunction (BHJ) OPVs.[1−20] Exciton dissociation occurs at the D/A interface, and selective hole and electron harvesting occur at the bottom and top contacts, respectively. Interlayers added at the contact/photoactive layer interface enhance selective harvesting of these charges. Interdigitation of donor/acceptor phases at small length scales ($2-3L_D$) provides for vectoral harvesting of photogenerated charges and active layers with high optical density.

OPV Device Platforms

Two OPV device configurations, planar heterojunction (PHJ) and bulk heterojunction (BHJ), are shown in panels A and B of Figure 1; in both technologies. oxide contacts play a critical role in determining device efficiencies. PIET in both PHJ and BHJ OPVs leads to charge separation (D^+/A^-) at the donor/acceptor interface; charges that escape recombination are collected at top and bottom electrodes, producing the photocurrent (J_{ph}). Rates of charge collection at the top and bottom contacts must be fast and hole- or electron-selective,[15] ensuring dark rectification of the *J*/*V* response, large values for J_{ph}, open-circuit photopotential (V_{oc}), high fill factors (FF), and high η.[3−11]

Exciton diffusion lengths (L_D) in many organic films are small, $\alpha L_D \approx 0.05$ (α = absorptivity (cm^{-1}), and active layer thickness in current PHJ OPVs may be only 20−60 nm.[11,16,17] Texturing the donor and acceptor layers in BHJ OPVs (Figure 1B) increases the D/A interfacial contact area, and well mixed films with domain sizes close to L_D increase J_{ph} and η.[1,2,5,6,11,18−20] Oxide films play a role in this texturing process (see below), and textured oxide layers can replaces one of the organic components in certain OPVs, acting as a transparent contact and electron acceptor/electron transport layer (A).[21,22] Frontier orbital energy offsets (Figure 2) at the O/O′ interface ($E_{HOMO}^{D} - E_{LUMO}^{A}$) set the upper limit to V_{oc},[3,4,7] while the offset $E_{LUMO}^{D} - E_{LUMO}^{A}$ controls rates of PIET and the short-circuit photocurrent J_{sc}.[4,7,23−25]

In the main portion of Figure 2, the local vacuum reference energy level is assumed constant at each interface in the OPV. Vacuum levels are rarely constant in multilayered devices, and in the upper portion of Figure 2, we show how these levels can shift at any one of the interfaces in the OPV, because of the introduction of interface dipoles at D/A heterojunctions,[26−29] or as a result of the introduction of modifiers at the interface between the TCO contact and organic.[20,24,29−34] Modifiers with electronegative substituents (e.g., fluorine) at their termini shift the local vacuum level to increase the effective work function. Modifiers with neutral or electron-donating substituents lower the effective work function.[31−33] These modifications affect both surface energy (wettability) of the contact and its effective work function and play a key role in charge collection in OPVs.

Achieving contact selectivity in OPVs is often achieved using "interlayers",[13−15,35−37] on the basis of conducting polymers, interposed between oxide contacts and donor layers (see below),[37−40] or ultra-thin films of alkali metal halides (e.g., LiF) and/or large band gap molecules, such as bathocuproine (BCP) or aluminum quinolate (Alq_3), added between electron acceptor layers and top metal contacts.[36,41] Interlayer materials, such as BCP and Alq_3, are "damaged" by certain evaporated metal films, and the "graphitic" products apparently mediate current flow across these interfaces.[41,42]

Diode equivalent circuits (see the conspectus), and various modifications to the Shockley equation have been used to model OPVs.[7,9,43]

$$J = J_o\left(\exp\left(\frac{V - JR_s}{n_o k_B T/e}\right) - 1\right) + \frac{V - JR_s}{R_p} - J_{ph} \qquad (1)$$

J is the total current (A/cm^2); J_o is the reverse saturation current, J_{ph} is the photocurrent, n_o is the ideality factor, and k_B, *T*, and *e* have their usual significance. Deviations from ideal diode behavior have been modeled using parasitic series and parallel (shunt) resistance terms (R_s and R_p), elevated values of n_o, and incorporation of a second shunt resistance and diode to model the OPV under illumination.[9] Values of R_p below ca. 10^4 Ω cm^2, are undesirable, arising typically from pinhole defects in extremely active layers, which can arise from incompatibility between polar oxide contacts and the nonpolar active layers (see below).[13,14,20,29,44] Low values of R_p may also be related to the field dependence of current arising from impurities within the organic layers and from thermionic (dark) injection of charge carriers at the D/A interface.[5,6,10]

Low values of R_s, the sum of resistances as a result of current flow in the thin metal and metal oxide contact thin films ($R_s = R_{s,TCO} + R_{s,TOP}$), less than ca. 1 Ω cm^2, are essential in efficient OPVs, placing a premium on the electrical properties of the oxide contacts. $R_{s,TCO}$ often determines the maximum size of individual OPV cells in an OPV array.[44,45] Some "champion" OPV efficiencies have been measured on selected small area cells; however, the efficiencies and lifetimes of practical OPV arrays must be quantified with cell areas of at least 1 cm^2.[45,46] Real improvements in OPV performance must be

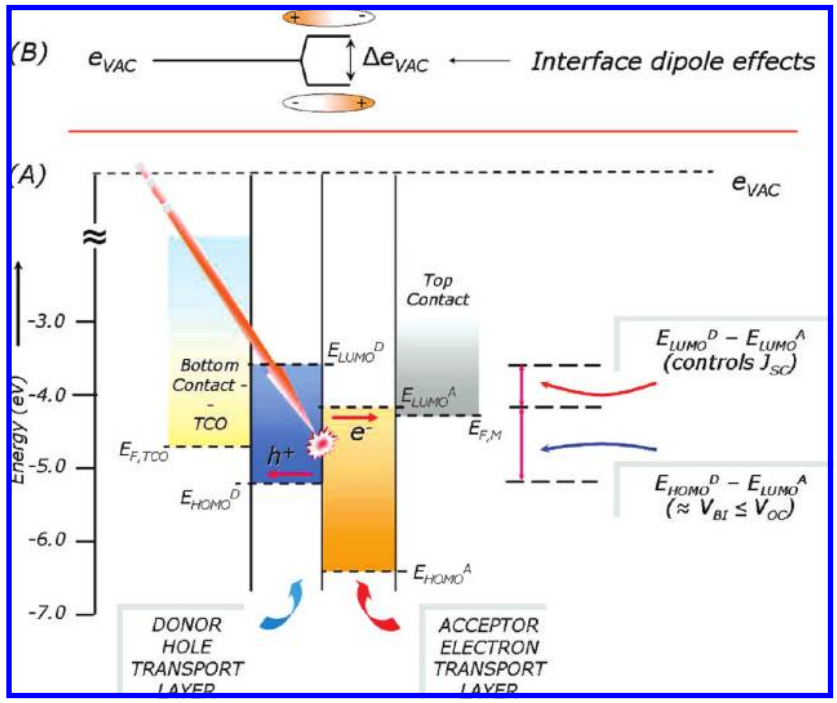

FIGURE 2. (A) Frontier orbital energy offsets in a planar organic heterojunction OPV,[8,23−34] assuming the local vacuum level is unchanged throughout the structure. V_{oc} is controlled by the energy offset $E_{HOMO}^{D} - E_{LUMO}^{A}$. The rate of PIET and J_{sc} are controlled by the energy offset $E_{LUMO}^{D} - E_{LUMO}^{A}$. (B) At each of the phase boundaries, the local vacuum level can shift because of interface dipoles at each heterojunction, affecting V_{oc}, rates of PIET, and rates of charge collection at organic/oxide or organic/metal heterojunctions.[7]

accompanied by studies that define the molecular origins of both R_s and R_p, as well as the field dependence of the photocurrent in both PHJ and BHJ OPVs.

It is not yet clear which modification strategies are needed to ensure chemically stable "ohmic" top and bottom contacts.[3,47] Modification strategies to enhance rates of solution electrochemical charge injection/collection, minimizing "contact resistance",[38,48−50] have led to improvements in OPV device performance; however, strategies that significantly increase the electroactive area (versus the geometric area) in TCO and related contact films are needed, as D/A layers are optimized and photocurrent densities increase. Fully optimized OPVs under AM 1.5 G illumination must ultimately demonstrate (i) good dark rectification ($J_{forward}/J_{reverse} \geq 1000$), (ii) low values of R_s and high values of R_p, with $n_o \approx 2$, and (iii) $0.5 \leq V_{oc} \leq 1$ V, short-circuit photocurrents, $J_{sc} \geq 15$ mA/cm^2, FF ≥ 0.65, and power conversion efficiencies, η, approaching 10% with only small changes in η during the lifetime of the device.

We focus here on interfacial chemistries and electronic properties of ITO, the most widely used bottom (and sometimes top) contact in OPVs, while alternative contact materials are sought.[44] ITO has excellent conductivity and transparency and will serve as a prototype contact until other alternatives are available. The issue of composition at metal/organic contacts is ignored in this Account but has been covered in several other recent reports.[23,51]

ITO and Related TCO Materials

Near-Surface Composition and Chemical Instabilities. Indium oxide (IO) is a wide bandgap ($E_{BG} \geq 3.5$ eV) insulator whose valence band arises mainly from O(2p) orbitals and whose conduction band arises from unfilled metal [In(5s)] orbitals (Figure 3). Electrical conductivity is introduced via interstitial tin dopants (Sn/In ratios up to 1:10) and removal of oxygen from the IO lattice,[52] producing electron-rich states near or within the conduction band (Figure 3B). Dopant densities of $10^{18}-10^{-20}$ cm^{-3} lead to resistivities of ca. $10^{-4}-10^{-3}$ Ω cm, sheet resistances of less than 15 Ω cm^2, with complex microcrystallinity, enhanced near-surface dopant concentrations, and substantial chemical reactivity in as-prepared films.[44,53]

The chemical reactivity of clean ITO has been recently reviewed, with special attention to the sites for dissociative chemisorption of H_2O.[54] The reactivity of clean ITO toward H_2O has been confirmed by X-ray photoelectron spectroscopy (XPS).[49,53,55,56] The known hydrolysis chemistries of metal oxides provide insights into the possible surface reactions of a wide range of TCOs.[57] Indium oxides, as with aluminum oxides, hydrolyze to $In(OH)_3$ and polynuclear products. These

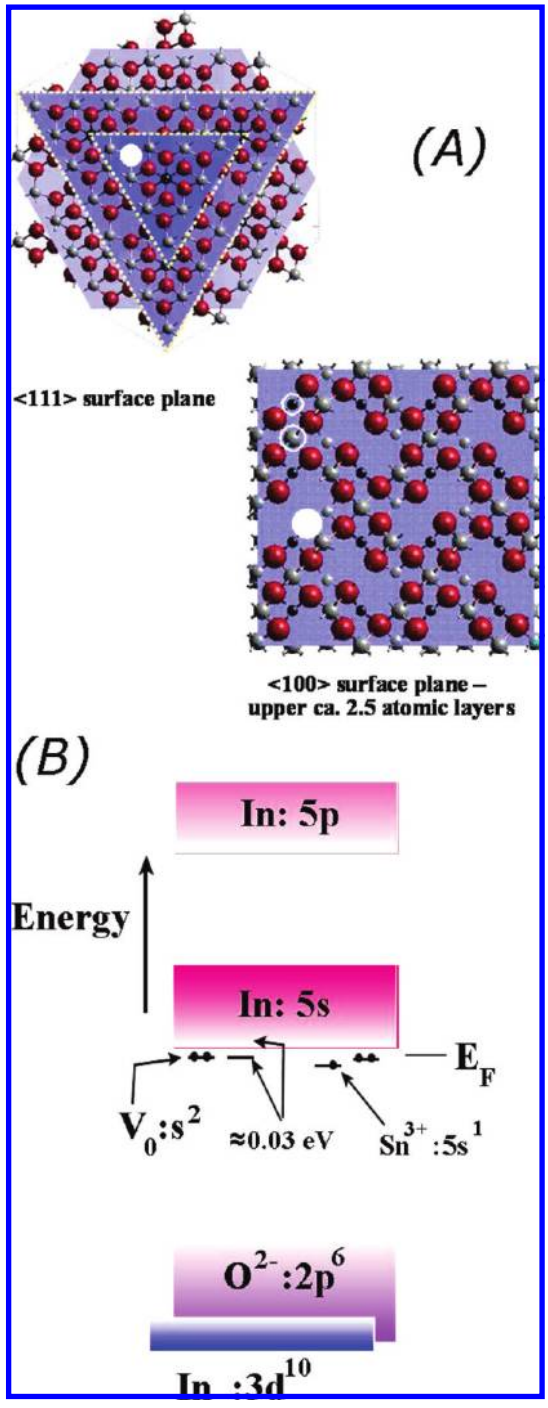

FIGURE 3. (A) In_2O_3 unit cell (bixebyte) showing the ⟨111⟩ and ⟨100⟩ terminations, with possible oxygen vacancies labeled in white.[44,52−57] (B) Band structure for Sn-doped In_2O_3 (ITO). Filled O(2p) orbitals comprise the VB, while unfilled In(5s) orbitals comprise the CB. Oxygen defects (V_O:s^2) creating donor levels ca. 0.03 eV below the conduction band edge, and electron-rich excess tin sites (Sn^{3+} and Sn^{2+}) introduce conductivity to the IO lattice.[52]

hydrolysis products have low solubilities and low conductivities, leading to uneven passivation of the ITO surface.

Alternative TCO materials under consideration include oxides of zinc, titanium, nickel, and trinary and ternary oxides.[13,44,58−60] Their stability toward hydrolysis and etching are balanced against abundance, cost, ease of processing, and ease of surface modification. Zinc oxide (ZO), an increasingly popular electron-transporting, easily textured TCO, is less stable toward hydrolysis than ITO. The hydrolysis products [species such as $Zn(OH)_2$] are "etched" in even slightly acidic environments.[57] Chemical modification of this oxide will be a key factor in the optimization of such contact materials, to both control polarity and chemical stability.[61] An appealing new TCO is indium−zinc oxide (IZO), deposited by sputtering at low processing temperatures onto glass or plastic.[58] IZO maintains the electrical properties of ITO, uses less indium, and forms smooth, amorphous films. To date, the surface chemistry of IZO in our hands is dominated by the same surface chemistries seen in ZO and modification with small molecules (see below) is promising.

Titanium oxides are appealing as electron-transport materials and as interlayers for the modification of other oxides.[22] They form self-limiting monolayer coverage hydroxides, with low solubilities of the hydroxide products.[57] ZO, modified by thin films of TiO_2, shows enhanced stabilities and has been used as a current collector in OPVs.[60] Titanium oxide films have been used as modifiers to ITO bottom contacts in BHJ OPVs with improved photopotentials and power conversion efficiencies.[13] Substoichiometric titanium oxides may find application as electrically conductive interlayers in tandem cell OPVs.[62] Such oxide layers must be "doped" with oxygen vacancies,[63] to function as recombination layers, and such substoichiometric oxides are likely to be unstable in OPVs requiring long lifetimes.

Near-Surface Electrical Heterogeneity. Non-uniform chemical reactivity and doping of ITO[64,65] leads to heterogeneous electrical properties on sub-micrometer length scales. Electrical heterogeneity of this type in silicon-based Schottky diodes, on sub-micrometer length scales, degrades device performance,[68] suggesting that similar effects may be seen in OPVs. SnO- and Sn_3O_4-like crystalline domains have been observed in highly doped ITO films and are likely to be sites of the highest electrical activity. Atomic force microscopy (AFM) and conductive tip AFM (C-AFM) have been used to confirm these heterogeneities in ITO electrodes, subjected to various cleaning/activation steps (Figure 4).[53] DSC−ITO corresponds to ITO cleaned in combinations of detergents, ethanol, and distilled water. OP−ITO is further cleaned/activated in oxygen RF plasmas (100−400 W),[66] producing surfaces with high work functions and more uniform electrical activity. ITO has also been subjected to brief exposures of concentrated HI or $HCl/FeCl_3$, both treatments previously used to

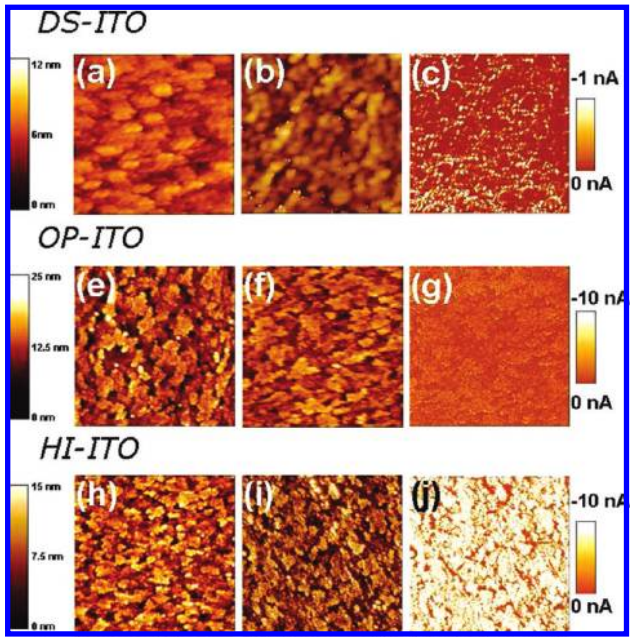

FIGURE 4. Images in a, e, and h are tapping mode AFM height images from conventional oxide-sharpened silicon nitride tips; images b, f, and i are height images using the boron-doped diamond tip; and images c, g, and j are current images from the same tip. Images a−c are for DSC−ITO; images e−g are for OP−ITO; and images h−j are for DSC−ITO etched with concentrated HI for 5−10 s. For image c, the tip bias was −1.0 V, while for images g and j, the tip bias was −0.02 V.[53]

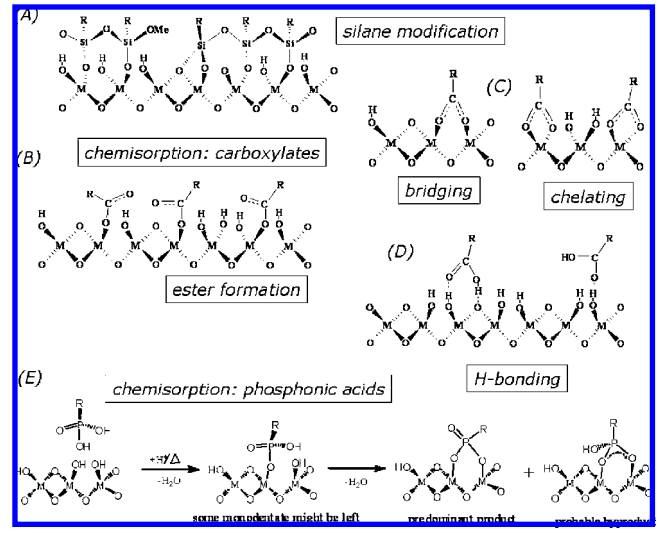

FIGURE 5. Modification schemes for metal oxide contacts. (A) Covalent modification using monolayers/multilayers of functional silanes; such modifiers control hole harvesting/injection rates and introduce electrically and electrochemical functional groups.[71,80,81] (B−D) Carboxylic acid chemisorption via bridging, chelation, ester formation and hydrogen bonding.[48−50,70] (E) Phosphonic acid chemisorption is a robust modification protocol, introducing functional groups that control work function and create oxide surfaces with low surface free energies and excellent wettabilities toward nonpolar organic layers.[32−34,75]

lithographically pattern ITO electrodes,[53] removing 1−10 nm from the ITO film.

In Figure 4c (tip bias = 1 V), electrical "hotspots" are discernible in DSC−ITO, confirming previous reports, where the existence of widely variable contamination layers ca. 3−5 nm in thickness were proposed.[67] For OP−ITO samples (Figure 4e), the ITO subgrain structure is observable and high contrast C-AFM current images (Figure 4g) are obtained with lower tip bias (ca. 20 mV). The uniformity of electrical response in OP−ITO films is striking, and OP−ITO electrodes in our hands have consistently provided the best PHJ OPV performance, for PHJ OPVs based on phthalocyanine donor layers.[20,29,69] The best electrical activity in C-AFM images is seen for ITO electrodes subjected to brief acid etching (Figure 4j). These surfaces are chemically reactive, and enhanced electrical activity is short-lived without chemical modification. For the electrochemical growth of conducting polymer layers, this treatment precedes the chemisorption of small molecules that function as "seed" layers for polymer growth and is an essential step in the creation of dense, electrically conductive layers.[38,50,70]

Chemical Modification with Small Molecules. Additional strategies have been developed to modify oxide surfaces to (i) lower their surface free energy, (ii) chemically stabilize these surfaces against hydrolysis and attack by acidic overlayers, (iii) tune their effective work functions, and (iv) enhance rates of electron transfer across their interfaces. No single modification strategy has simultaneously achieved all of these goals.

Figure 5 summarizes modification strategies for ITO and related oxides.[38,48−50,55,61,71] Silanes (Figure 5A) create brush-like or cross-linked, stable mono- to multilayer films on a variety of oxides.[61,71] Small-molecule chemisorption (panels B−E of Figure 5) is easier to implement for TCO films.[32−34,38,48−50,55] Chemisorbed carboxylic acids can be introduced (panels B−D of Figure 5) via chelation, ester formation, electrostatic interactions, or hydrogen bonding.[72] Some carboxylates "etch" oxide surfaces, such as ITO, IZO, etc.,[49] leading to enhanced surface coverages of electroactive groups and rates of electron transfer, with concomitant improvements in device performance for organic light-emitting diodes (OLEDs) and PHJ OPVs.[48,49]

Phosphonic acids (PA) lead to robust monolayers via mono-, bi-, and tridentate binding modes (Figure 5E). Together with the groups of Marder and Brédas, we have recently chemisorbed a variety of PAs to ITO surfaces (Figure 6), with the intent of controlling both surface work function and surface free energy.[32−34] Changes in the effective surface work function and local vacuum level shifts, monitored with UV-photoelectron spectroscopy (UPS), showed similar work function changes to those seen for coinage metals modified with

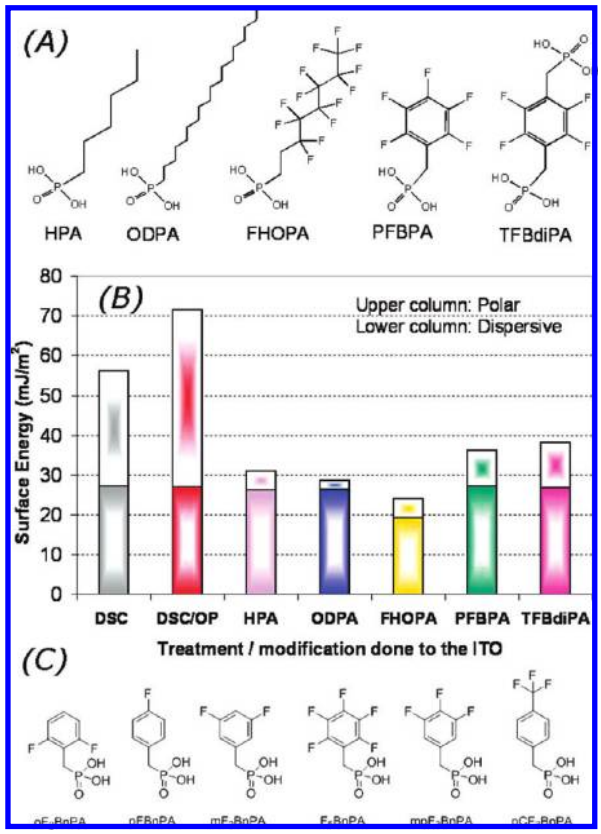

FIGURE 6. Phosphonic acid oxide modifiers, providing for a wide range of effective work function and surface free energy. (A and C) Alkane, fluorinated alkane, and fluorinated aryl PA modifiers. (B) Surface energy (mJ/m^2) from contact-angle studies, as a function of the modifier. Both polar (upper column) and dispersive interactions (lower column) are shown (adapted from refs 32−34).

alkanethiol self-assembled monolayers.[31,73] The shift in effective work function per unit change in dipole moment ($\Delta\varphi/\Delta D$ = ca. −0.4 eV ± 0.05 eV/Debye) is nearly the same for Au, Ag, and ITO, consistent with models for these modifiers that separate the dipole moment of the main molecular fragment from the bond dipole of the attachment group.[74] Contact-angle studies showed that both the polar and dispersive contributions to surface energy area are affected by PA modification (Figure 6).[32−34] PA modification in general lowers the surface energy of OP−ITO, making it more wettable by nonpolar organic layers. Fluorinated alkyl and fluorinated aryl PAs simultaneously increase the effective work function of ITO to values higher than seen for clean Au. Such modifications lead to improvements in both OLED and OPV devices using PA-modified TCOs, shown by Kippelen and co-workers.[10,75]

Electrochemical Modification with Ultra-thin Conducting Polymer Films. TCOs can be modified using spin-cast[76] or electrochemically grown[38,48,50,77] hole-selective conducting polymer "interlayers" between the oxide and the donor layer of an OPV or OLED (Figure 1). Spin-cast thin films of

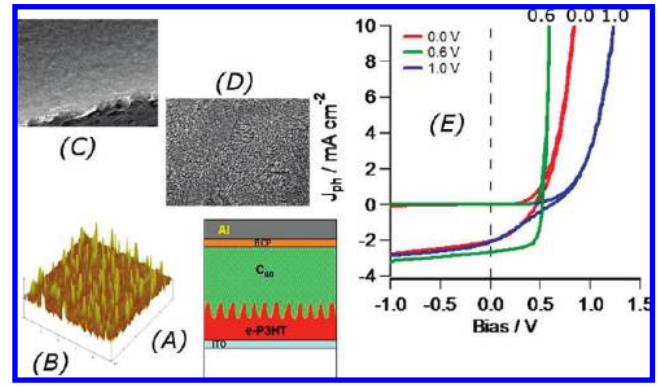

FIGURE 7. (A) OPVs created from electrodeposited poly(3-hexylhtiophene) (e-P3HT)-textured e-P3HT layers are deposited on HI−ITO electrodes, using a thiophene carboxylic acid "seed layer". C_{60} electron-acceptor layers are vacuum-deposited over the textured polymer film. (B) AFM image (2 × 2 μm) and (C and D) FE-SEM images (0.5 × 0.5 μm) showing smooth or textured e-P3HT layers possible on nanometer-length scales. (E) *J*/*V* response for ITO/e-P3HT/C_{60}/BCP/Al OPVs as a function of the "doping potential" (0.0, 0.6, and 1.0 V) in the e-P3HT layer. Fill factors, FF ≥ 0.65, are achieved with e-P3HT layers that are partially doped and optimally conductive (adapted from ref 50).

poly(ethyleneoxythiophene) with poly(styrenesulfonate) (PEDOT:PSS) (i) planarize the oxide film, (ii) increase contact compatibility with nonpolar organic layers, and (iii) increase the effective surface work function.[45,78] Recent C-AFM studies, however, suggest that electrical non-uniformity remains in PEDOT:PSS films,[76,79] and the sulfonate groups, with effective pK_a values near 1.0, decrease the stability of oxide contacts.

Conducting polymer layers [PEDOT and poly(3-hexylthiophenes), e-PEDOT and e-P3HT], with electrical properties surpassing PEDOT:PSS, can be grown on acid-activated, small-molecule-modified ITO, with excellent control of thickness and microstructure.[38,50] Using probe molecules, such as ferrocene (Fc) and dimethylferrocene (DMFc), ITO electrodes optimized with e-PEDOT and e-P3HT films demonstrated heterogeneous electron-transfer rates (k_{ET}) enhanced by factors up to $10^4\times$ over unmodified ITO and factors of 10−100× over ITO modified with PEDOT:PSS. Marks and co-workers also recently demonstrated self-assembled or cross-linked polymer layers on ITO, with excellent electroactivity and selectivity for hole-harvesting, and may provide contact stability not seen for PEDOT:PSS thin films.[80,81]

Electrodeposited poly(3-hexylthiophene) (e-P3HT) films (Figure 7) are also photoelectrically active, demonstrating photovoltaic activity as components of e-PEHT/C_{60} heterojunctions.[50] Pulsed potential electrodeposition produces dense, pinhole-free e-P3HT "carpet layers" or nanotextured polymer layers (panels A and B of Figure 7). e-P3HT/C_{60} OPVs (Figure 7C)

showed modest efficiencies for white light (100 mW/cm^2) illumination, with good incident photon current efficiencies. Nearly the same J_{sc} values were seen for each film type; however, their FF values are strongly controlled by the degree of postdeposition doping of the polymer, demonstrating how the electrical properties of the ITO/organic interface control both FF and η. Electrodeposition protocols are now pursued for OPVs requiring patterned poly(thiophene) layers and to produce host polymers for semiconductor nanoparticles.[70]

Nanotextured (TiOPc/C_{60}) OPVs Using Unmodified ITO Substrates. The high surface energy of OP−ITO,[32−34] making it poorly wettable by nonpolar layers, may provide a route to tuning the microstructural characteristics of certain vacuum deposited organic layers, such as titanyl phthalocyanine (TiOPc) (Figure 8).[20] TiOPc and related Pc's undergo phase transformations that extend their photoactivity well into the near-IR,[82,83] and as shown in Figure 8D, as-deposited 2−20 nm thickness "Phase I" TiOPc films on OP−ITO are conformal, with the subgrain structure of the underlying ITO substrate observable in both AFM and scanning electron microscopic images. "Solvent annealing" of the Pc film promotes the Phase I → Phase II phase transformation,[84,85] release of the surface tension in as-deposited films, and "nanotexturing" of these solvent-annealed Pc layers [panels F and G of Figure 8 (ITO substrates) and panels I and J of Figure 8 (Si(100) substrates)], and ITO/TiOPc/C_{60}/BCP/Al OPVs show a ca. 2× enhancement in Pc/C_{60} interfacial area, photocurrent response, and device efficiency.[20] AM 1.5 G power conversion efficiencies, estimated from incident photon current efficiency data (IPCE), for both Phase I and II TiOPc/C_{60} heterojunctions, were 1.1 and 2.2%, respectively, and recent studies in our group suggest that OPV efficiencies will be further enhanced by simple modifications to ITO surface chemistry, the electron affinity of the acceptor, and enhancements in thin-film structures that raise FF. For some donor layers, control of surface polarity of contact materials will control microstructure in a wider variety of donor/acceptor heterojunctions. These studies also point to a potential problem in OPV optimization: slow dewetting of an oxide contact may occur spontaneously for many organic donor or acceptor layers, and interfacial layers that physically, chemically, and electronically stabilize these thin films for prolonged operational periods, at high temperatures, will be essential.

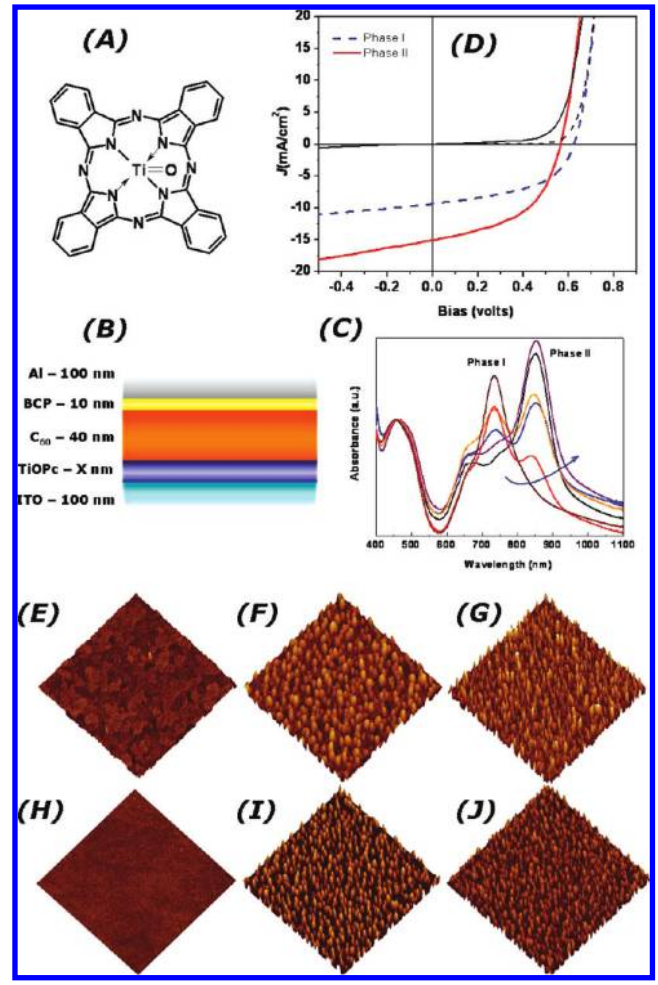

FIGURE 8. (A) Titanyl phthalocyanine (TiOPc) donor layers vacuum deposited on OP−ITO to create (B) TiOPc/C_{60} OPVs. (C) *Q*-band absorbance spectra during the Phase I → Phase II transformation of TiOPc. (D) *J*/*V* dark and light (100 mW/cm^2) behavior for OPVs based on ITO/TiOPc (20 nm)/C_{60} (40 nm)/BCP (10 nm)/Al devices, with 100% phase I or 100% phase II TiOPc layers. (E and F) AFM images (2 × 2 μm) of 2 nm films of TiOPc on ITO before and after solvent annealing. (G) Film (20 nm) of TiOPc on ITO after solvent annealing. (H−J) Comparable coverages of TiOPc on smooth Si(100). Initially deposited (phase I) TiOPc layers are conformal with the surface and are textured after solvent annealing (adapted from ref 20).

Conclusions

At the center of the scientific issues that must be addressed to bring OPVs to full commercialization is the problem of interfacing disparate materials (oxides or metals) with nonpolar organic layers. Solutions to this problem require understanding and control of surface composition and the energetics of electron transfer, at nanometer-length scales. Single monolayers and multilayers of molecular modifiers at oxide/organic interfaces will have a significant impact on properties such as work function, polarity, and mediation of electron transfer. To fully optimize device performance, these parameters will have to be optimized simultaneously, in robust formats. The challenges to develop viable OPV technologies are in some respects greater than those for other organic electronic technologies because they operate at full sunlight and elevated

temperatures. ITO will clearly be the contact of choice for early generation OPVs, but more earth-abundant oxides or even nonoxides will likely take its place. Characterization and modification protocols developed for this prototype TCO are likely to extrapolate to a much broader range of thin-film contact materials.

This research has been supported over the last several years by the National Science Foundation (CHE-0517963, the NSF Science and Technology Center, Materials and Devices for Information Technology, DMR-0120967), the Office of Naval Research, the Department of Energy Program, "Photovoltaics Beyond the Horizon" (NREL), the Basic Energy Sciences division of the Department of Energy (DE-FG03-02ER15378 and DE-FG03-02ER15753), and the Arizona Board of Regents TRIF program, Arizona Research Institute for Solar Energy (AzRISE). We extend our thanks to the many collaborators who made this research possible over the least several years, including Carrie Donley, Chet Carter, Saneeha Marrikar, Weining Wang, Dana Alloway, Wei Xia, Thomas Schulmeyer, Ken Nebesny, Paul Lee, Simon Jones, Sergio Paniagua, Seunghyup Yoo, Benoit Domercq, Peter Hotchkiss, Seth Marder, Jean-Luc Brédas, and Bernard Kippelen.

BIOGRAPHICAL INFORMATION

Neal R. Armstrong has been Professor of Chemistry Optical Sciences at the University of Arizona since 1978. His research interests range from the creation and characterization of new materials for energy conversion, light emission and sensing, to the characterization of the critical interfaces in these technologies.

P. Alex Veneman is a Ph.D. graduate student at the University of Arizona (anticipated completion in 2009). His B.S. degree was in materials science and engineering from Cornell University (2003).

Erin Ratcliff is a postdoctoral fellow at the University of Arizona. Her Ph.D. degree was in physical chemistry (Iowa State University in 2007) preceded by a B.A. degree in chemistry, mathematics, and statistics (St. Olaf College in 2003).

Diogenes Placencia is a graduate student at the University of Arizona, since 2005. His B.S. and M.S. degrees came from Sacred Heart University in Fairfield, CT.

Michael T. Brumbach is currently a staff scientist at Sandia National Laboratories. He received his Ph.D. degree in chemistry from the University of Arizona in 2007 and his M.S. degree in materials science and engineering from Alfred University in 2002.

FOOTNOTES

*To whom correspondence should be addressed. E-mail: nra@email.arizona.edu.

REFERENCES

1 Dennler, G.; Scharber, M. C.; Brabec, C. J. Polymer−fullerene bulk-heterojunction solar cells. *Adv. Mater.* **2009**, *21*, 1323–1338.

2 Brabec, C. J.; Durrant, J. R. Solution-processed organic solar cells. *MRS Bull.* **2008**, *33*, 670–675.

3 Gregg, B. A.; Hanna, M. C. Comparing organic to inorganic photovoltaic cells: Theory, experiment, and simulation. *J. Appl. Phys.* **2003**, *93*, 3605–3614.

4 Scharber, M. C.; Wuhlbacher, D.; Koppe, M.; Denk, P.; Waldauf, C.; Heeger, A. J.; Brabec, C. L. Design rules for donors in bulk-heterojunction solar cells—Towards 10% energy-conversion efficiency. *Adv. Mater.* **2006**, *18*, 789–794.

5 McNeill, C. R.; Westenhoff, S.; Groves, C.; Friend, R. H.; Greenham, N. C. Influence of nanoscale phase separation on the charge generation dynamics and photovoltaic performance of conjugated polymer blends: Balancing charge generation and separation. *J. Phys. Chem. C* **2007**, *111*, 19153–19160.

6 Blom, P. W. M.; Mihailetchi, V. D.; Koster, L. J. A.; Markov, D. E. Device physics of polymer:fullerene bulk heterojunction solar cells. *Adv. Mater.* **2007**, *19*, 1551–1566.

7 Rand, B. P.; Burk, D. P.; Forrest, S. R. Offset energies at organic semiconductor heterojunctions and their influence on the open-circuit voltage of thin-film solar cells. *Phys. Rev. B: Condens. Matter Mater. Phys.* **2007**, *75*, 115327-1–115327-11.

8 Forrest, S. R. The limits to organic photovoltaic cell efficiency. *MRS Bull.* **2005**, *30*, 28–32.

9 Yoo, S.; Domercq, B.; Kippelen, B. Intensity-dependent equivalent circuit parameters of organic solar cells based on pentacene and C-60. *J. Appl. Phys.* **2005**, *97*, 9.

10 Potscavage, W. J.; Yoo, S.; Kippelen, B. Origin of the open-circuit voltage in multilayer heterojunction organic solar cells. *Appl. Phys. Lett.* **2008**, *93*, 3.

11 Yang, F.; Forrest, S. R. Photocurrent generation in nanostructured organic solar cells. *ACS Nano* **2008**, *2*, 1022–1032.

12 Reese, M. O.; Morfa, A. J.; White, M. S.; Kopidakis, N.; Shaheen, S. E.; Rumbles, G.; Ginley, D. S. Pathways for the degradation of organic photovoltaic P3HT:PCBM based devices. *Sol. Energy Mater. Sol. Cells* **2008**, *92*, 746–752.

13 Steim, R.; Choulis, S. A.; Schilinsky, P.; Brabec, C. J. Interface modification for highly efficient organic photovoltaics. *Appl. Phys. Lett.* **2008**, *92*, 3.

14 Steim, R.; Choulis, S. A.; Schilinsky, P.; Lemmer, U.; Brabec, C. J. Formation and impact of hot spots on the performance of organic photovoltaic cells. *Appl. Phys. Lett.* **2009**, *94*, 3.

15 Bisquert, J.; Cahen, D.; Hodes, G.; Ruhle, S.; Zaban, A. Physical chemical principles of photovoltaic conversion with nanoparticulate, mesoporous dye-sensitized solar cells. *J. Phys. Chem. B* **2004**, *108*, 8106–8118.

16 Shaw, P. E.; Ruseckas, A.; Samuel, I. D. W. Exciton diffusion measurements in poly(3-hexylthiophene). *Adv. Mater.* **2008**, *20*, 3516–3520.

17 Yoo, S.; Potscavage, W. J.; Domercq, B.; Han, S. H.; Li, T. D.; Jones, S. C.; Szoszklewicz, R.; Levi, D.; Riedo, E.; Marder, S. R.; Kippelen, B. Analysis of improved photovoltaic properties of pentacene/C-60 organic solar cells: Effects of exciton blocking layer thickness and thermal annealing. *Solid-State Electron.* **2007**, *51*, 1367–1375.

18 Kim, Y.; Cook, S.; Tuladhar, S. M.; Choulis, S. A.; Nelson, J.; Durrant, J. R.; Bradley, D. D. C.; Giles, M.; McCulloch, I.; Ha, C. S.; Ree, M. A strong regioregularity effect in self-organizing conjugated polymer films and high-efficiency polythiophene:fullerene solar cells. *Nat. Mater.* **2006**, *5*, 197–203.

19 Ma, W. L.; Yang, C. Y.; Gong, X.; Lee, K.; Heeger, A. J. Thermally stable, efficient polymer solar cells with nanoscale control of the interpenetrating network morphology. *Adv. Funct. Mater.* **2005**, *15*, 1617–1622.

20 Placencia, D.; Wang, W.; Shallcross, R. C.; Nebesny, K. W.; Brumbach, M.; Armstrong, N. R. Organic photovoltaic cells based on solvent-annealed, textured titanyl phthalocyanine/C_{60} heterojunctions. *Adv. Funct. Mater.* **2009**, *19*, 1913–1921.

21 Olson, D. C.; Lee, Y. J.; White, M. S.; Kopidakis, N.; Shaheen, S. E.; Ginley, D. S.; Voigt, J. A.; Hsu, J. W. P. Effect of ZnO processing on the photovoltage of ZnO/poly(3-hexylthiophene) solar cells. *J. Phys. Chem. C* **2008**, *112*, 9544–9547.

22 Liu, D.; Yang, P. Y.; Luscombe, C. K. Preparation of titanium oxide pillars on glass substrates and ultrathin titanium oxide layer using PMMA/PS blend films. *J. Phys. Chem. C* **2008**, *112*, 7886–7894.

23 Zahn, D. R. T.; Gavrila, G. N.; Salvan, G. Electronic and vibrational spectroscopies applied to organic/inorganic interfaces. *Chem. Rev.* **2007**, *107*, 1161–1232.

24 Armstrong, N. R.; Wang, W.; Alloway, D.; Placencia, D.; Ratcliff, E.; Brumbach, M. Organic/organic′ heterojunctions: Organic light emitting diodes and organic photovoltaic devices. *Macromol. Rapid Commun.* **2009**, *30*, 717–731.

25 Alloway, D. M.; Armstrong, N. R. Characterization of the heterojunctions formed between phthalocyanines and perylene dyes by UV and X-ray photoelectron spectroscopies. *Appl. Phys. A: Mater. Sci. Process.* **2009**, *95*, 209–218.

26 Chen, W.; Huang, H.; Chen, S.; Huang, Y. L.; Gao, X. Y.; Wee, A. T. S. Molecular orientation-dependent ionization potential of organic thin films. *Chem. Mater.* **2008**, *20*, 7017–7021.

27 Vazquez, H.; Gao, W.; Flores, F.; Kahn, A. Energy level alignment at organic heterojunctions: Role of the charge neutrality level. *Phys. Rev. B: Condens. Matter Mater. Phys.* **2005**, *71*, 041306.

28 Molodtsova, O. V.; Knupfer, M. Electronic properties of the organic semiconductor interfaces CuPc/C-60 and C-60/CuPc. *J. Appl. Phys.* **2006**, *99*, 053704.

29 Brumbach, M.; Placencia, D.; Armstrong, N. R. Titanyl phthalocyanine/C-60 heterojunctions: Band-edge offsets and photovoltaic device performance. *J. Phys. Chem. C* **2008**, *112*, 3142–3151.

30 Cahen, D.; Kahn, A. Electron energetics at surfaces and interfaces: Concepts and experiments. *Adv. Mater.* **2003**, *15*, 271–277.

31 Alloway, D. M.; Hofmann, M.; Smith, D. L.; Gruhn, N. E.; Graham, A. L.; Colorado, R.; Wysocki, V. H.; Lee, T. R.; Lee, P. A.; Armstrong, N. R. Interface dipoles arising from self-assembled monolayers on gold: UV-photoemission studies of alkanethiols and partially fluorinated alkanethiols. *J. Phys. Chem. B* **2003**, *107*, 11690–11699.

32 Paramonov, P. B.; Paniagua, S. A.; Hotchkiss, P. J.; Jones, S. C.; Armstrong, N. R.; Marder, S. R.; Bredas, J.-L. Theoretical characterization of the indium tin oxide surface and of its binding sites for adsorption of phosphonic acid monolayers. *Chem. Mater.* **2008**, *20*, 5131–5133.

33 Paniagua, S. A.; Hotchkiss, P. J.; Jones, S. C.; Marder, S. R.; Mudalige, A.; Marrikar, F. S.; Pemberton, J. E.; Armstrong, N. R. Phosphonic acid modification of indium−tin oxide electrodes: Combined XPS/UPS/contact angle studies. *J. Phys. Chem. C* **2008**, *112*, 7809–7817.

34 Hotchkiss, P. J.; Li, H.; Paramonov, P. B.; Paniagua, S. A.; Jones, S. C.; Armstrong, N. R.; Brédas, J.-L.; Marder, S. R. Modification of the surface properties of ITO with benzylphosphonic acids: A joint experimental and theoretical study. *Adv. Mater.* **2009**, *21*, 1–6.

35 Hanisch, J.; Ahlswede, E.; Powalla, M. Contacts for semitransparent organic solar cells. *Eur. Phys. J.: Appl. Phys.* **2007**, *37*, 261–264.

36 Brabec, C. J.; Shaheen, S. E.; Winder, C.; Sariciftci, N. S.; Denk, P. Effect of LiF/metal electrodes on the performance of plastic solar cells. *Appl. Phys. Lett.* **2002**, *80*, 1288–1290.

37 Peisert, H.; Petr, A.; Dunsch, L.; Chasse, T.; Knupfer, M. Interface fermi level pinning at contacts between PEDOT:PSS and molecular organic semiconductors. *ChemPhysChem* **2007**, *8*, 386–390.

38 Marrikar, F. S.; Brumbach, M.; Evans, D. H.; Lebron-Paler, A.; Pemberton, J. E.; Wysocki, R. J.; Armstrong, N. R. Modification of indium−tin oxide electrodes with thiophene copolymer thin films: Optimizing electron transfer to solution probe molecules. *Langmuir* **2007**, *23*, 1530–1542.

39 Tengstedt, C.; Kanciurzewska, A.; de Jong, M. P.; Braun, S.; Salaneck, W. R.; Fahlman, M. Ultraviolet light-ozone treatment of poly(3,4-ethylenedioxy-thiophene)-based materials resulting in increased work functions. *Thin Solid Films* **2006**, *515*, 2085–2090.

40 Hwang, J.; Amy, F.; Kahn, A. Spectroscopic study on sputtered PEDOT·PSS: Role of surface PSS layer. *Org. Electron.* **2006**, *7*, 387–396.

41 Gommans, H.; Verreet, B.; Rand, B. P.; Muller, R.; Poortmans, J.; Heremans, P.; Genoe, J. On the role of bathocuproine in organic photovoltaic cells. *Adv. Funct. Mater.* **2008**, *18*, 3686–3691.

42 Davis, R. J.; Pemberton, J. E. Investigation of the interfaces of tris-(8-hydroxyquinoline) aluminum with Ag and Al using surface Raman spectroscopy. *J. Phys. Chem. C* **2008**, *112*, 4364–4371.

43 Green, M. A. *Solar Cells: Operation Principles, Technology, And System Applications*; Prentice-Hall: Englewood, NJ, 1982; pp 63−101.

44 Fortunato, E.; Ginley, D.; Hosono, H.; Paine, D. C. Transparent conducting oxides for photovoltaics. *MRS Bull.* **2007**, *32*, 242–247.

45 Cravino, A.; Schilinsky, P.; Brabec, C. J. Characterization of organic solar cells: The importance of device layout. *Adv. Funct. Mater.* **2007**, *17*, 3906–3910.

46 Shrotriya, V.; Li, G.; Yao, Y.; Moriarty, T.; Emery, K.; Yang, Y. Accurate measurement and characterization of organic solar cells. *Adv. Funct. Mater.* **2006**, *16*, 2016–2023.

47 Shen, Y. L.; Hosseini, A. R.; Wong, M. H.; Malliaras, G. G. How to make ohmic contacts to organic semiconductors. *ChemPhysChem* **2004**, *5*, 16–25.

48 Armstrong, N. R.; Carter, C.; Donley, C.; Simmonds, A.; Lee, P.; Brumbach, M.; Kippelen, B.; Domercq, B.; Yoo, S. Y. Interface modification of ITO thin films: Organic photovoltaic cells. *Thin Solid Films* **2003**, *445*, 342–352.

49 Carter, C.; Brumbach, M.; Donley, C.; Hreha, R. D.; Marder, S. R.; Domercq, B.; Yoo, S.; Kippelen, B.; Armstrong, N. R. Small molecule chemisorption on indium−tin oxide surfaces: Enhancing probe molecule electron-transfer rates and the performance of organic light-emitting diodes. *J. Phys. Chem. B* **2006**, *110*, 25191–25202.

50 Ratcliff, E. L.; Jenkins, J. L.; Nebesny, K.; Armstrong, N. R. Electrodeposited "nano-textured" poly(3-hexyl-thiophene) (e-P3HT) films for photovoltaic applications. *Chem. Mater.* **2008**, *20*, 5796–5806.

51 Hwang, J.; Wan, A.; Kahn, A. Energetics of metal-organic interfaces: New experiments and assessment of the field. *Mater. Sci. Eng., R* **2009**, *64*, 1–31.

52 Warschkow, O.; Miljacic, L.; Ellis, D. E.; Gonzalez, G. B.; Mason, T. O. Interstitial oxygen in tin-doped indium oxide transparent conductors. *J. Am. Ceram. Soc.* **2006**, *89*, 616–619.

53 Brumbach, M.; Veneman, P. A.; Marrikar, F. S.; Schulmeyer, T.; Simmonds, A.; Xia, W.; Lee, P.; Armstrong, N. R. Surface composition and electrical and electrochemical properties of freshly deposited and acid-etched indium tin oxide electrodes. *Langmuir* **2007**, *23*, 11089–11099.

54 Zhou, C. G.; Li, J. Y.; Chen, S.; Wu, J. P.; Heier, K. R.; Cheng, H. S. First-principles study on water and oxygen adsorption on surfaces of indium oxide and indium tin oxide nanoparticles. *J. Phys. Chem. C* **2008**, *112*, 14015–14020.

55 Donley, C.; Dunphy, D.; Paine, D.; Carter, C.; Nebesny, K.; Lee, P.; Alloway, D.; Armstrong, N. R. Characterization of indium−tin oxide interfaces using X-ray photoelectron spectroscopy and redox processes of a chemisorbed probe molecule: Effect of surface pretreatment conditions. *Langmuir* **2002**, *18*, 450–457.

56 Gassenbauer, Y.; Klein, A. Electronic and chemical properties of tin-doped indium oxide (ITO) surfaces and ITO/ZnPc interfaces studied in-situ by photoelectron spectroscopy. *J. Phys. Chem. B* **2006**, *110*, 4793–4801.

57 Baes, C. F., Jr.; Mesmer, R. E. *The Hydrolysis of Cations*; John Wiley and Sons: New York, 1976; pp 319−327, 349−357.

58 Taylor, M. P.; Readey, D. W.; van Hest, M.; Teplin, C. W.; Alleman, J. L.; Dabney, M. S.; Gedvilas, L. M.; Keyes, B. M.; To, B.; Perkins, J. D.; Ginley, D. S. The remarkable thermal stability of amorphous In−Zn−O transparent conductors. *Adv. Funct. Mater.* **2008**, *18*, 3169–3178.

59 Irwin, M. D.; Buchholz, B.; Hains, A. W.; Chang, R. P. H.; Marks, T. J. p-Type semiconducting nickel oxide as an efficiency-enhancing anode interfacial layer in polymer bulk-heterojunction solar cells. *Proc. Natl. Acad. Sci. U.S.A.* **2008**, *105*, 2783–2787.

60 Olson, D. C.; Shaheen, S. E.; White, M. S.; Mitchell, W. J.; van Hest, M.; Collins, R. T.; Ginley, D. S. Band-offset engineering for enhanced open-circuit voltage in polymer-oxide hybrid solar cells. *Adv. Funct. Mater.* **2007**, *17*, 264–269.

61 Allen, C. G.; Baker, D. J.; Albin, J. M.; Oertli, H. E.; Gillaspie, D. T.; Olson, D. C.; Furtak, T. E.; Collins, R. T. Surface modification of ZnO using triethoxysilane-based molecules. *Langmuir* **2008**, *24*, 13393–13398.

62 Kim, J. Y.; Lee, K.; Coates, N. E.; Moses, D.; Nguyen, T. Q.; Dante, M.; Heeger, A. J. Efficient tandem polymer solar cells fabricated by all-solution processing. *Science* **2007**, *317*, 222–225.

63 Diebold, U. The surface science of titanium dioxide. *Surf. Sci. Rep.* **2003**, *48*, 53–229.

64 Nakao, T.; Nakada, T.; Nakayama, Y.; Miyatani, K.; Kimura, Y.; Saito, Y.; Kaito, C. Characterization of indium tin oxide film and practical ITO film by electron microscopy. *Thin Solid Films* **2000**, *370*, 155–162.

65 Kobayashi, T.; Kimura, Y.; Suzuki, H.; Sato, T.; Tanigaki, T.; Saito, Y.; Kaito, C. Process of crystallization in thin amorphous tin oxide film. *J. Cryst. Growth* **2002**, *243*, 143–150.

66 Kim, J. S.; Friend, R. H.; Cacialli, F. Surface energy and polarity of treated indium−tin oxide anodes for polymer light-emitting diodes studied by contact-angle measurements. *J. Appl. Phys.* **1999**, *86*, 2774–2778.

67 Liau, Y. H.; Scherer, N. F.; Rhodes, K. Nanoscale electrical conductivity and surface spectroscopic studies of indium−tin oxide. *J. Phys. Chem. B* **2001**, *105*, 3282–3288.

68 Sullivan, J. P.; Tung, R. T.; Pinto, M. R.; Graham, W. R. Electron-transport of inhomogeneous Schottky barriers—A numerical study. *J. Appl. Phys.* **1991**, *70*, 7403–7424.

69 Veneman, A.; Armstrong, N. R. Spatially resolved current spectroscopy (SCS) at the nanometer scale: Imaging electrical heterogeneity in contacts for molecular electronics. *ACS Nano* **2009**, in press.

70 Shallcross, R. C.; D'Ambruoso, G. D.; Korth, B. D.; Hall, H. K.; Zheng, Z. P.; Pyun, J.; Armstrong, N. R. Poly(3,4-ethylenedioxythiophene)—Semiconductor nanoparticle composite thin films tethered to indium tin oxide substrates via electropolymerization. *J. Am. Chem. Soc.* **2007**, *129*, 11310–11311.

71 Veinot, J. G. C.; Marks, T. J. Toward the ideal organic light-emitting diode. The versatility and utility of interfacial tailoring by cross-linked siloxane interlayers. *Acc. Chem. Res.* **2005**, *38*, 632–643.

72 Gratzel, M. Dye-sensitized solar cells. *J. Photochem. Photobiol., C* **2003**, *4*, 145–153.

73 Alloway, D.; Graham, A.; Yang, X.; Mudalige, A.; Wysocki, V. W.; Pemberton, J. E.; Lee, T. R.; Colorado, R., Jr.; Wysocki, R.; Armstrong, N. R. Tuning the effective work function of gold and silver using ω-functionalized alkanethiols: Varying surface composition through dilution and choice of terminal groups *J. Phys. Chem. C* **2009**, in press.

74 Heimel, G.; Romaner, L.; Zojer, E.; Bredas, J.-L. The interface energetics of self-assembled monolayers on metals. *Acc. Chem. Res.* **2008**, *41*, 721–729.

75 Sharma, A.; Kippelen, B.; Hotchkiss, P. J.; Marder, S. R. Stabilization of the work function of indium tin oxide using organic surface modifiers in organic light-emitting diodes. *Appl. Phys. Lett.* **2008**, *93*, 163308.

76 Pingree, L. S. C.; MacLeod, B. A.; Ginger, D. S. The changing face of PEDOT:PSS films: Substrate, bias, and processing effects on vertical charge transport. *J. Phys. Chem. C* **2008**, *112*, 7922–7927.

77 Berlin, A.; Vercelli, B.; Zotti, G. Polythiophene- and polypyrrole-based mono- and multilayers. *Polym. Rev.* **2008**, *48*, 493–530.

78 Greczynski, G.; Kugler, T.; Keil, M.; Osikowicz, W.; Fahlman, M.; Salaneck, W. R. Photoelectron spectroscopy of thin films of PEDOT—PSS conjugated polymer blend: A mini-review and some new results. *J. Electron Spectrosc. Relat. Phenom.* **2001**, *121*, 1–17.

79 Pingree, L. S. C.; Reid, O. G.; Ginger, D. S. Electrical scanning probe microscopy on active organic electronic devices. *Adv. Mater.* **2009**, *21*, 19–28.

80 Li, J. F.; Wang, L.; Liu, J.; Evmenenko, G.; Dutta, P.; Marks, T. J. Characterization of transparent conducting oxide surfaces using self-assembled electroactive monolayers. *Langmuir* **2008**, *24*, 5755–5765.

81 Hains, A. W.; Marks, T. J. High-efficiency hole extraction/electron-blocking layer to replace poly(3,4-ethylenedioxythiophene):poly(styrene sulfonate) in bulk-heterojunction polymer solar cells. *Appl. Phys. Lett.* **2008**, *92*, 023504.

82 Klofta, T. J.; Danziger, J.; Lee, P.; Pankow, J.; Nebesny, K. W.; Armstrong, N. R. Photoelectrochemical and spectroscopic characterization of thin-films of titanyl phthalocyanine—Comparisons with vanadyl phthalocyanine. *J. Phys. Chem.* **1987**, *91*, 5646–5651.

83 Coppede, N.; Toccoli, T.; Pallaoro, A.; Siviero, F.; Walzer, K.; Castriota, M.; Cazzanelli, E.; Iannotta, S. Polymorphism and phase control in titanyl phthalocyanine thin films grown by supersonic molecular beam deposition. *J. Phys. Chem. A* **2007**, *111*, 12550–12558.

84 Mizuguchi, J.; Rihs, G.; Karfunkel, H. R. Solid-state spectra of titanylphthalocyanine as viewed from molecular distortion. *J. Phys. Chem.* **1995**, *99*, 16217–16227.

85 Conboy, J. C.; Olson, E. J. C.; Adams, D. M.; Kerimo, J.; Zaban, A.; Gregg, B. A.; Barbara, P. F. Impact of solvent vapor annealing on the morphology and photophysics of molecular semiconductor thin films. *J. Phys. Chem. B* **1998**, *102*, 4516–4525.